

Microwave, Photo- and Thermally Responsive PNIPAm–Gold Nanoparticle Microgels

Bridgette M. Budhlall,^{*,†,‡,§} Manuel Marquez,[§] and Orlin D. Velev^{*,‡}

NSF funded Center for High-Rate Nanomanufacturing and Nanomanufacturing Center of Excellence,
Department of Plastics Engineering, University of Massachusetts, Lowell, Massachusetts 01854,
Department of Chemical and Biomolecular Engineering, North Carolina State University,
Raleigh, North Carolina 27695, NIST Center for Theoretical and Computational Nanosciences,
Gaithersburg, Maryland 20899, Harrington Department of Bioengineering, Arizona State University,
Tempe, Arizona, and Center for Integrated Nanotechnologies,
Los Alamos National Laboratory, Los Alamos, New Mexico 87545

Received June 21, 2008. Revised Manuscript Received August 22, 2008

Microwave-, photo- and thermo-responsive polymer microgels that range in size from 500 to 800 μm and are swollen with water were prepared by a novel microarray technique. We used a liquid–liquid dispersion technique in a system of three immiscible liquids to prepare hybrid PNIPAm-co-AM core–shell capsules loaded with AuNPs. The spontaneous encapsulation is a result of the formation of double oil-in-water-in-oil (o/w/o) emulsion. It is facilitated by adjusting the balance of the interfacial tensions between the aqueous phase (in which a water-soluble drug may be dissolved), the monomer phase and the continuous phase. The water-in-oil (w/o) droplets containing 26 wt% NIPAm and Am monomers, 0.1 wt% Tween-80 surfactant, FITC fluorescent dye and colloidal gold nanoparticles spontaneously developed a core–shell morphology that was fixed by in situ photopolymerization. The results demonstrate new reversibly swelling and deswelling AuNP/PNIPAm hybrid core–shell microcapsules and microgels that can be actuated by visible light and/or microwave radiation (≤ 1250 nm) and/or temperature. This is the first study to demonstrate that incorporating AuNPs speeds up the response kinetics of PNIPAm, and hence enhances the sensitivity to external stimuli of PNIPAm. These microgels can have potential applications for microfluidic switches or microactuators, photosensors, and various nanomedicine applications in controlled delivery and release.

Introduction

The objectives of this research are first, to better understand the fundamental principles of liquid–liquid phase separation¹ inside emulsion droplets and multiple emulsions² (O/W/O) and second, to employ these principles to synthesize *stimuli*-responsive metallic nanoparticle-polymer composite microgels. Microgels with *stimuli*-responsive controlled release systems will have potential applications to accommodate transport and delivery of molecules (e.g., drugs, beneficial agents, and genes), and may act as sensors and/or actuators. Depending on the molecule to be encapsulated a variety of approaches are possible. Specific characteristics, such as rigidity and elasticity of the polymer capsule wall, substrate recognition (both chemi- and physisorption) and triggered release or disintegration (e.g., pH, temperature) need to be taken into account.

Considerable attention has been given to delivery vehicles containing gold nanoparticles (AuNPs). A number of methods have been developed to incorporate gold nanoparticles and various polymer molecules. Combining the sensitivity of a *stimuli*-responsive polymer with inorganic metal nanoparticles results in hybrid composite microgels with attractive synergistic properties. Depending on the nature of inorganic metal incor-

porated as nanoparticles, such as Au, Cu, Fe and Ag, specific functionality can be realized for potential applications in micro/nano sensors or microreactors, nanoelectric devices,³ in photothermal ablation of cancer tumors⁴ and in perspective drug delivery and release applications.⁵

Poly(*N*-isopropylacrylamide) (PNIPAm)⁶ is a *stimuli*-responsive polymer which when swollen with water, exhibit a pH-, temperature-, or light-responsive volume phase transition⁷ that is accompanied by a sharp coil-to-globule transition of the polymer chains at the so-called lower critical solution temperature (LCST) at approximately 32 °C in the aqueous phase.⁸

(3) (a) Chu, L. Y.; Park, S. H.; Yamaguchi, T.; Nakao, S. *J. Membr. Sci.* **2001**, *192*, 27–39. (b) Sauer, M.; Streich, D.; Meier, W. *Adv. Mater.* **2001**, *13*, 1649–1651. (c) Nardin, C.; Widmer, J.; Winterhalter, M.; Meier, W. *Eur. Phys. J.* **2001**, *4*, 403–410. (d) Zhang, Q.; Remsen, E. E.; Wooley, K. L. *J. Am. Chem. Soc.* **2000**, *122*, 3642–3651. (e) Ibarz, G.; Dahne, L.; Donath, E.; Möhwald, H. *Adv. Mater.* **2001**, *13*, 1324–1327. (f) Sukhorukov, G. B.; Antipov, A. A.; Voigt, A.; Donath, E.; Möhwald, H. *Macromol. Rapid Commun.* **2001**, *22*, 4, 4–6. (g) Lu, Y.; Mei, M.; Dechler, M.; Ballauff, M. *Angew. Chem.* **2006**, *118*, 827–830. *Angew. Chem. Int. Ed.* **2006**, *45*, 843–816. (h) Fu, Q.; Rama Rao, G. V.; Ward, T. L.; Lu, Y.; Lopez, G. P. *Langmuir* **2007**, *23*, 170–174.

(4) Sershen, S. R.; Westcott, S. L.; Halas, N. J.; West, J. L. *J. Biomed. Mater. Res.* **2000**, *51*, 293–298.

(5) (a) Gorelikov, I.; Field, L. M.; Kumacheva, E. *J. Am. Chem. Soc.* **2004**, *126*, 15938–15939. (b) Zhang, H.; Mardiyani, S.; Chan, W. C. W.; Kumacheva, E. *Biomacromolecules* **2006**, *7*, 1568–1572. (c) Das, M.; Mardiyani, S.; Chan, W. C. W.; Kumacheva, E. *Adv. Mater.* **2006**, *18*, 80–83. (d) Das, M.; Sanson, N.; Fava, D.; Kumacheva, E. *Langmuir* **2007**, *23*, 196–201.

(6) Schild, H. G. *Prog. Polym. Sci.* **1992**, *17*, 163–249.

(7) (a) Hirotsu, S.; Hirokawa, Y.; Tanaka, T. *J. Chem. Phys.* **1987**, *87*, 1392–1395. (b) Siegel, R. A.; Firestone, B. A. *Macromolecules* **1988**, *21*, 3254–3259. (c) Suzuki, A.; Tanaka, T. *Nature* **1990**, *346*, 345–347. (d) Saunders, B. R.; Vincent, B. *Adv. Colloid Interface Sci.* **1999**, *80*, 1–25. (e) Garcia, A.; Marquez, M.; Cai, T.; Rosario, R.; Hu, Z.; Gust, D.; Hayes, M.; Vail, S. A.; Park, C.-D. *Langmuir* **2007**, *23*, 224–229.

(8) (a) Tanaka, T. *Phys. Rev. Lett.* **1980**, *45*, 1636–1639. (b) Pelton, R. H.; Pelton, H. M.; Morpheus, A.; Rowell, R. L. *Langmuir* **1989**, *5*, 816–818. (c) Schild, H. G.; Tirrell, D. A. *J. Phys. Chem.* **1990**, *94*, 4352–4356.

* To whom correspondence should be addressed. E-mail: bridgette_budhlall@uml.edu (B.M.B.); odvelev@unity.ncsu.edu (O.D.V.).

[†] University of Massachusetts.

[‡] North Carolina State University.

[§] NIST Center for Theoretical and Computational Nanosciences, Arizona State University, and Los Alamos National Laboratory.

(1) (a) Loxley, A.; Vincent, B. *J. Colloid Interface Sci.* **1998**, *208*, 49–62. (b) Dowding, P. J.; Atkin, R.; Vincent, B.; Bouillot, P. *Langmuir* **2004**, *20*, 11374–11379. (c) Dowding, P. J.; Atkin, R.; Vincent, B.; Bouillot, P. *Langmuir* **2005**, *21*, 5278–5284.

(2) Opawale, F. O.; Burgess, D. J. *J. Pharm. Pharmacol.* **1998**, *50*, 965–973.

Various techniques have been proposed for the preparation of core-shell microcapsules using *stimuli*-responsive polymers, for instance, layer-by-layer (LbL) deposition, phase separation, construction of colloidosomes, interfacial polymerization and RAFT precipitation polymerization coupled with microwave synthesis.^{9–15} Several challenges remain in the core-shell fabrication process, including controlling the stability of the colloid and attaining high yield with controlled size and morphology of the microcapsules. The process should also include a few steps and be inexpensive. Microcapsules synthesized with a core-shell morphology using thermo-responsive PNIPAm as the polymer shell are an attractive structure because of their ability to carry substances within their core for drug delivery and release applications.¹⁶

The incorporation of inorganic metal nanoparticles into organic polymer to prepare hybrid composite microgels provides novel properties as compared to the pure PNIPAm polymer. Metal nanoparticles that have been incorporated in hybrid composite PNIPAm microgels include Ag,^{3g} silica,¹⁷ iron¹⁸ and Au.⁴ The metallic nanoparticles are embedded either in the core cavity or the polymer shell, immobilized either by physical entanglement¹⁹ or covalent bonding.²⁰

AuNPs in particular, have received wide attention especially in the design of new drug delivery vehicles because gold is a bioinert material that will not induce an adverse bioreaction if it becomes detached from the microcapsule polymer. Colloidal AuNPs are optically active materials whereby varying the particle size and shape allows its surface plasmon resonance (SPR) frequency to be tuned over the visible and near-infrared (NIR) spectrum.²¹ Radiation in controlled doses can be used for *in vivo* imaging because of minimal light absorption by hemoglobin

(>650 nm) and water (<900 nm).²² Radiation between 650 nm and ~1250 nm can thus be safely used to excite the AuNP at its resonance frequency. The adsorption of the light energy by the AuNPs will generate heat locally within the polymer microcapsule shell; when the temperature increases to or above LCST, the microgel will collapse or shrink resulting in a release of any chemical species contained inside the capsule. PNIPAm microgels have gained attention for use in drug delivery applications.^{4,5}

In the present study, no purification is necessary in the process of synthesis of microwave and light actuated microgel particles. This synthesis and the characterization of the microgel properties are facilitated by a novel, simple microarray-based water-in-oil (w/o) inverse emulsion technique.

It was decided rather than developing a system that dissipates heat using high-intensity laser pulses, to evaluate the microwave response of AuNP-loaded poly(*N*-isopropylacrylamide-*co*-acrylamide) [AuNP/PNIPAm-*co*-Am]. These microgels have not been previously investigated and should, in principle, absorb microwave radiation at a higher rate than the environment, locally heat the microgel and surrounding media in isolated microvolumes to temperatures that are well below the pain threshold,^{22a} solvent vaporization and melting or fragmentation of the AuNPs.²³ Due to the high efficiency of microwave heating, microwave-assisted chemical synthesis has attracted recent attention,^{24a} and microwave-assisted heating could accelerate the rates of polymerization reaction^{24b} and improve the properties of products.^{24c}

The goal of this study was to develop a robust technique to synthesize a hybrid composite core-shell microgel that can be activated in a controlled manner by visible light *and* microwave radiation to release the liquid contained in the cores. To achieve this goal, we incorporated AuNPs into a polymer matrix comprised of NIPAm copolymerized with a hydrophilic monomer, acrylamide (Am), which has been shown to increase the LCST.⁸ The monomer ratios are adjusted to obtain a LCST closer to the physiological conditions (37 °C) modeling systems required for drug, protein, gene or cell delivery and controlled release applications.

Recently we reported a simple one-step liquid-liquid dispersion technique to synthesize reversibly swellable, magnetic nanoparticles-embedded polymer microcapsules.²⁵ In the present method, we utilized this liquid-liquid dispersion principle²⁵ in a system of 3 immiscible liquids to prepare PNIPAm-*co*-AM core-shell microcapsules loaded with AuNPs. The core-shell morphology was developed *in situ* and fixed by photopolymerization by using a novel microarray technique. Our results demonstrated the development for the first time to the best of the authors' knowledge, AuNP/PNIPAm hybrid core-shell microcapsules and microgels that can be actuated by visible light and/or microwave radiation (≤ 125 mm) and/or temperature. These results are significant first, because the microarray technique is rapid and robust and can be scaled up relatively easily for producing commercial quantities of AuNP/PNIPAm-*co*-Am microcapsules and microgels and second, because the liquid core of the polymer microcapsule can be released by activation by a range of electromagnetic radiation or temperature.

(9) (a) Caruso, F.; Caruso, R. A.; Mohwald, H. *Science* **1998**, *282*, 1111–1114. (b) Donath, E.; Sukhorukov, G. B.; Davis, S. A.; Möhwald, H. *Angew. Chem., Int. Ed.* **1998**, *37*, 2201–2205. (c) Antipov, A. A.; Sukhorukov, G. B.; Donath, E.; Möhwald, H. *J. Phys. Chem. B* **2001**, *105*, 2281–2284. (d) Peyratout, C. S.; Dahne, L. *Angew. Chem., Int. Ed.* **2004**, *43*, 3762–3783.

(10) (a) Loxley, A.; Vincent, B. J. *Colloid Interface Sci.* **1998**, *208*, 49–62. (b) Shulkin, A.; Stöver, H. D. H. *Macromolecules* **2003**, *36*, 9836–9839. (c) Dowding, P. J.; Atkin, R.; Vincent, B.; Bouilliot, P. *Langmuir* **2004**, *20*, 11374–11379.

(11) (a) Velev, O. D.; Furusawa, K. *Langmuir* **1996**, *12*, 2374–2384. (b) Dinsmore, A. D.; Mink, F.; Hsu, M. G.; Marquez, M.; Bausch, A. R.; Weitz, D. A. *Science* **2002**, *298*, 1006–1009. (c) He, X. D.; Ge, X. W.; Lui, H. R.; Wang, M. Z.; Zhang, Z. C. *Chem. Mater.* **2005**, *17*, 5891–5892.

(12) (a) Pham, H. H.; Kumacheva, E. *Macromol. Symp.* **2003**, *192*, 191–205. (b) Chu, L. Y.; Xie, R.; Zhu, J. H.; Chen, W. M.; Yamaguchi, T.; Nakao, S. J. *Colloid Interface Sci.* **2003**, *265*, 187–196.

(13) (a) Nakagawa, K.; Iwamoto, S.; Nakajima, M.; Shono, A.; Satoh, K. J. *Colloid Interface Sci.* **2004**, *278*, 198–205. (b) Quek, C. H.; Li, J.; Sun, T.; Ling, M.; Chan, H.; Mao, H. Q.; Gan, L. M.; Leong, K. W.; Yu, H. *Biomaterials* **2004**, *25*, 3531–3540.

(14) (a) Hotz, J.; Meier, W. *Langmuir* **1998**, *14*, 1031–1036. (b) Utada, A. S.; Lorenceau, E.; Link, D. R.; Kaplan, P. D.; Stone, H. A.; Weitz, D. A. *Science* **2005**, *308*, 537–541. (c) Nie, Z.; Xu, S.; Seo, M.; Lewis, P. C.; Kumacheva, E. *J. Am. Chem. Soc.* **2005**, *127*, 8058–8063.

(15) (a) An, Z.; Shi, Q.; Tang, W.; Tsung, C.-K.; Hawker, C. J.; Stucky, G. D. *J. Am. Chem. Soc.* **2007**, *129*, 14493–1499. (b) An, Z.; Tang, W.; Hawker, C. J.; Stucky, G. D. *J. Am. Chem. Soc.* **2006**, *128*, 15054–15055.

(16) (a) Hsiue, G. H.; Hsu, S. H.; Yang, C. C.; Lee, S. H.; Yang, I. K. *Biomaterials* **2002**, *23*, 457–462. (b) Zhang, X. Z.; Wu, D. Q.; Chu, C. C. *Biomaterials* **2004**, *25*, 3793–3805.

(17) (a) Boukari, H.; Long, G. G.; Harris, M. T. *J. Colloid Interface Sci.* **2000**, *229*, 129–139. (b) Green, D. L.; Lin, J. S.; Lam, Y.-F.; Hu, M. Z.; Schaefer, D. W.; Harris, M. T. *J. Colloid Interface Sci.* **2003**, *266*, 346–358. (c) Karg, M.; Samtos, I. P.; MarZan, L. M. L.; Hellweg, T. *Chem. Phys. Chem.* **2006**, *7*, 2298–2301. (18) Deng, Y.; Yang, W.; Wang, C.; Fu, S. *Adv. Mater.* **2003**, *15*, 1729–1732.

(19) Ichia, L. S. H.; Sharabi, G.; Willner, I. *Adv. Funct. Mater.* **2002**, *12*, 27–32.

(20) Zhao, X.; Ding, X.; Deng, Z.; Zheng, Z.; Peng, Y.; Long, X. *Macromol. Rapid Commun.* **2005**, *26*, 1784–1787.

(21) (a) El-Sayed, M. A. *Acc. Chem. Res.* **2001**, *34*, 257–264. (b) Averitt, R. D.; Westcott, S. L.; Halas, N. J. *J. Opt. Soc. Am. B* **1999**, *182*, 4–1832. (c) Averitt, R. D.; Sarkar, D.; Halas, N. J. *Phys. Rev. Lett.* **1997**, *78*, 4217–4220. (d) Xia, Y.; Halas, N. J. *MRS Bull.* **2005**, *30*, 338–343.

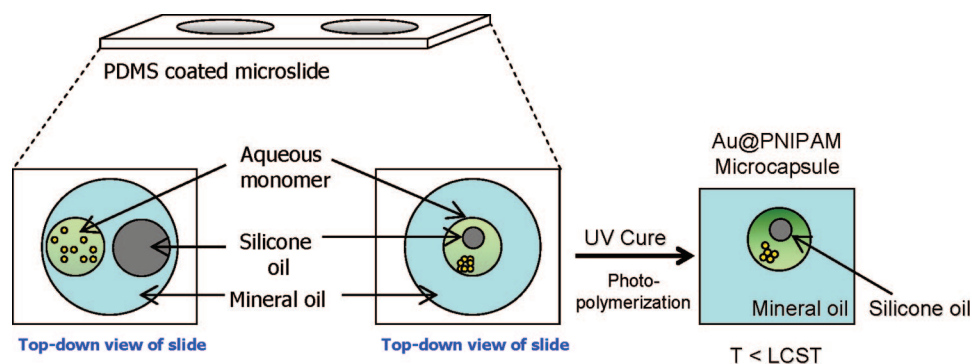
(22) (a) Weissleder, R. *Nat. Biotechnol.* **2001**, *19*, 316–317. (b) Simpson, C. R.; Kohl, M.; Essenpreis, M.; Cope, M. *Phys. Med. Biol.* **1998**, *43*, 2465–2478.

(23) Roper, D. K.; Ahn, W.; Hoepfner, M. *J. Phys. Chem. C* **2007**, *111*, 3636–3641.

(24) (a) Kappe, C. O. *Angew. Chem., Int. Ed.* **2004**, *43*, 6250–6284. (b) Murry, M.; Charlesworth, D.; Swires, L.; Riby, P.; Cook, J.; Chowdhry, B. Z.; Snowden, M. J. *J. Chem. Soc., Faraday Trans.* **1994**, *90*, 1999–2000. (c) Singh, V.; Tiwari, A.; Devendra, D. N.; Sanghi, R. *Carbohydr. Polym.* **2004**, *58*, 1–6.

(25) Koo, H. Y.; Chang, S. T.; Choi, W. S.; Park, J.-H.; Kim, D. Y.; Velev, O. D. *Chem. Mater.* **2006**, *18*, 3308–3313.

Scheme 1. Microarray w/o Emulsion Technique for the Synthesis of Gold/Polymer Core–Shell Microcapsules and Microgels



Experimental Section

Materials. Gold tetrachloroaurate trihydrate (HAuCl_4), sodium citrate, tannic acid, *N*-isopropylacrylamide (NIPAm), acrylamide (Am); and *N,N'*-methylene acrylamide (BIS) were purchased from Sigma-Aldrich, Milwaukee, WI. The NIPAm was purified by recrystallization from a 2:1 solvent mixture of *n*-hexane and toluene. A fluorescent dye, Fluorescein isothiocyanate (FITC) was used to label the polymer microgel. All other chemicals were used as-received.

Synthesis of Microcapsules Loaded with Gold Nanoparticles. NIPAm was copolymerized with Am in a 95:5 molar ratio (NIPAm-*co*-Am). Am was used as a copolymer because it has been shown to increase the LCST of the resulting PNIPAm-*co*-Am copolymer closer to biological temperatures. In order to increase the molecular weight and for the copolymer to be water-insoluble, BIS was added as a cross-linker in a 1:750 molar ratio (cross-linker/monomer).²⁶ Moderate solids content was present at 26 wt% monomer concentration. Varying aliquots of concentrated AuNPs, stabilized with a 0.1 wt% Tween-80 surfactant were added to the monomer solution and mixed. A photoinitiator, 2,2-dimethoxy-2-phenylacetophenone was added to give 1500 ppm concentration in solution. Higher concentrations of photoinitiator up to 4500 ppm were used in the photopolymerization of the light-responsive microgels. Photopolymerization was performed using a Black Ray UV lamp with a 100W Hg bulb at 365 nm wavelength for 30 min to 2 h for the microwave and thermoresponsive microgels and 15 min for the photoresponsive microgels. Equivalent PNIPAm-*co*-AM microgels without AuNPs were also prepared to serve in control experiments. The DI water used was obtained from Millipore RiOs 16 reverse osmosis water purification system (Bedford, MA).

Microarray Slide Assembly Preparation. We developed a simple microarray-type technique of inserting a small oil droplet in a larger static water drop contained in a concave well on a microslide, allowing real-time observations of the encapsulation process, of the polymerization processes and of the response of the microgels, respectively, in small volumes under the optical microscope. The technique for synthesis of the hybrid composite AuNP/PNIPAm-*co*-Am *microcapsule* (3 liquid phases) is illustrated in Scheme 1. Synthesis of *microgel* (2 liquid phases) particles in the absence of silicon oil was initially conducted as a proof-of-concept experiment. Biological hanging-drop glass microslides with two concavities 18 mm in diameter and 0.5 mm deep from Fisher Scientific (PA) were used as substrates ($25 \times 75 \times 2 \text{ mm}^3$ with frosted end). Thorough cleaning and oxidation was used to ensure clean surfaces. The slides were washed with Sparkleen detergent (Fisher Scientific), rinsed with DI water, dried overnight in an oven at 60–70 °C, and immersed in a Nochromix solution (Godax Laboratories, Tacoma Park, MD) for a minimum of 2 h. The slides were then thoroughly rinsed with DI water and dried again before being coated with poly(dimethylsily-

loxane) (PDMS) elastomer Sylgard 184²⁷ and curing agent (Dow Corning) to render their surfaces hydrophobic. Aqueous droplets (1 μL) containing monomers, initiator, colloidal AuNPs and fluorescent dye (FITC) are placed on the surface of a medium viscosity, high density mineral oil in each concavity of the microslide. The droplets initially sink into the oil and serve as self-contained microreactors which are then photopolymerized in situ under the UV lamp. These micron-sized emulsion droplets are photopolymerized into hybrid composite AuNP/PNIPAm-*co*-Am microgels after ~30–50 min of UV irradiation. The microgels are at least 500 μm in diameter and the processes of encapsulation, core ejection, and phase separation can be easily observed under the optical microscope.

Characterization. Imaging. The microgels were observed and their size and shape were characterized by optical microscopy (Olympus BX 61) with a digital charge-coupled device (CCD) camera (Olympus DP 70) with objective magnifications ranging from 4 \times to 50 \times . The microgels were continuously monitored from the top while being exposed to the external stimuli (light, microwave and temperature). A thermal stage was used to keep the microgels at a constant temperature while video images were captured using a DSC-V1 Cyber-Shot digital camera, SONY, Japan, coupled with the microscope.

Light Irradiation. The variation in size and shape of the microgels with visible light was monitored by exposure to varying number of light cycles, *n*, by alternating between a phase-contrast filter and a bright-field filter under an optical microscope. Micrograph images were taken for measurements of the diameter of the microcapsule under the phase-contrast filter (dark) obtained after 5 min to allow the microgel particles to reach equilibrium, following 5 min exposure to the bright-field filter (light) respectively. Under the dark-field, phase-contrast and bright-field filters, the wavelength of irradiation is within the visible region, while using the 100 W Hg lamp through the fluorescent filter, the wavelength of irradiation is 365–565 nm.

Microwave Irradiation. A commercially available 56.6 m³ capacity microwave oven operating at a maximum power level of 800 W and frequency of 2.45 GHz was used in this study. The microgels were exposed at a fixed microwave wavelength of 122 mm for increasing times (15–180 s) corresponding to increasing microwave energy dose of 0.21–2.54 kJ/m³ and images were recorded for measurements of the diameter of the microgel after each exposure.

Heating. The variation in microgel size with temperature was measured by heating on a hot plate. The temperature was increased a typical heating rate of 1 °C/min, allowing the temperature to equilibrate for 5 min each time prior to taking images for diameter measurements.

Results and Discussion

Synthesis of AuNP/PNIPAm-*co*-Am Hybrid Composite Microcapsules and Microgels. The first major challenge was finding three immiscible fluids one of which serves as a solvent

(26) Serchen, S.; Mensing, G.; Ng, M.; Halas, N.; Beebe, D.; West, J. *Adv. Mater.* **2005**, *17*, 1368–1372.

(27) Sold as Sylgard 184 by Dow Corning. See http://www.dowcorning.com/applications/product_finder/pf_details.asp?1=009&pg=0000029&prod=01064291&type=PROD for product details.

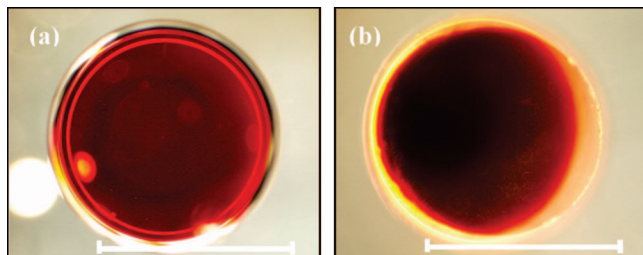


Figure 1. Optical micrographs of water-in-oil (w/o) droplet containing 26 wt% NIPAm and Am monomers, 0.1 wt% Tween-80 surfactant, FITC fluorescent dye and colloidal gold nanoparticles are shown in Figure 1 (a) before polymerization and (b) after 15 min of photopolymerization by UV exposure. The appearance of the droplet before polymerization (a) is uniformly red in color. After polymerization begins, the outer perimeter of the droplet polymerizes first. The appearance of the droplet after 15 min of polymerization is a dark red core surrounded by a transparent PNIPAm-*co*-Am polymer shell (b).

for the monomer and all three were nonsolvents for the polymer, facilitating phase-separation as the polymerization proceeds. In addition, PNIPAm-*co*-Am must also still display a LCST in the solvent-nonsolvent mixture. We screened a number of solvent-nonsolvent pairs and arrived at a formulation including water, silicone oil and mineral oil as a basis for 3-phase-separations to prepare *microcapsules* and used water and mineral oil as a basis for 2-phase separation to prepare *microgels*. Here we report only on the results for the synthesis and characterization of AuNP/PNIPAm-*co*-Am *microgel* particles prepared with a continuous phase of either mineral oil or water via an emulsion process facilitated by the microarray technique. The results for the 3-phase experiments as a basis to prepare *microcapsules* are reported in another publication.²⁸

The optical micrographs of water-in-oil (w/o) droplet containing 26 wt% NIPAm and Am monomers, 0.1 wt% Tween-80, FITC fluorescent dye and colloidal gold nanoparticles are shown in Figure 1 (a) before polymerization and (b) after 15 min of photopolymerization by UV exposure. The appearance of the droplet before polymerization (Figure 1a) is uniformly red in color. After polymerization begins, the outer perimeter of the droplet polymerizes first. The appearance of droplet after 15 min of polymerization is a dark red core surrounded by a transparent PNIPAm-*co*-Am polymer shell (Figure 1b).

PNIPAm exhibits a lower critical solution temperature LCST of 31–32 °C in water above which it precipitates upon heating.^{4,29} In the present study it was found that the LCST of homopolymerized PNIPAm is slightly lower than body temperature at 32.5 °C. However, LCST can be varied by copolymerization. It has been reported³⁰ that the incorporation of a hydrophilic monomer-acrylamide raised LCST of the PNIPAm gel. By varying the wt% hydrophilic monomer one can adjust the LCST in the range of 32–65 °C. In the current study, acrylamide was incorporated to achieve a PNIPAm-*co*-Am microgel with LCST in the target temperature range of 38–41 °C which is above the physiological body temperature of 37 °C but below the pain threshold of 42 °C.^{22a}

A summary of the experiments performed for w/o inverse emulsion AuNP/PNIPAm-*co*-Am microgel under different external stimuli is shown in Table 1.

Effect of Temperature. The effect of temperature on PNIPAm-*co*-Am microgels dispersed in a continuous phase of water with

Table 1. Experimental Parameters and Observations for w/o Emulsion AuNP/PNIPAm-*co*-Am Microgel under Different External Stimuli

external stimuli	property	without AuNPs	low AuNPs loading	high AuNPs loading
temperature (in water)	final particle size	same	N/A	same
	deswelling behavior	minimal (delta 5.4%)	N/A	extensive (delta 19%)
light	final particle size	larger (delta 6%)	N/A	smaller (delta 28%)
	deswelling behavior	minimal	N/A	extensive
microwave (in oil)	final particle size	larger (delta 7%)	medium (delta 16%)	smaller (delta 33%)
	deswelling behavior	minimal	moderate	extensive
microwave (in water)	final particle size	larger	medium	smaller (2×)
	deswelling behavior	moderate	extensive	extensive

and without AuNPs loading was characterized. The loading of AuNPs incorporated into the PNIPAm-*co*-Am was fixed at 10.3×10^{-4} g. The *normalized difference in diameter* of the PNIPAm-*co*-Am with and without loaded AuNPs in water as a function of temperature is plotted in Figure 2. Each microgel particle is normalized to its initial size because each microgel particle is not perfectly spherical. Hence three diameter measurements were taken at different points on the particle (top, middle, bottom) and an average of these measurements were calculated.

The phase transition temperature and the sharpness of the phase transition of the AuNP/PNIPAm-*co*-Am microgel are almost the same as those of the control PNIPAm-*co*-Am microgel. Since the microgels were polymerized for the same length of time, it can be assumed that they possess similar molecular weights (MW) and similar polymer chain lengths, and it can be expected that the LCST for microgels with and without AuNPs is the same.

The *normalized difference in diameter* is used to determine the *extent of shrinkage* of each microgel. For a greater *extent of shrinkage* the *normalized difference in diameter* (measured relative to the initial size) is higher and vice versa. It was observed that both microgels decreased with increasing temperature. However, in the temperature range of 25–40 °C, the presence of AuNPs increases the *extent of shrinkage* of the PNIPAm-*co*-Am microgels from 5.4% to 19%. Since the measurement is

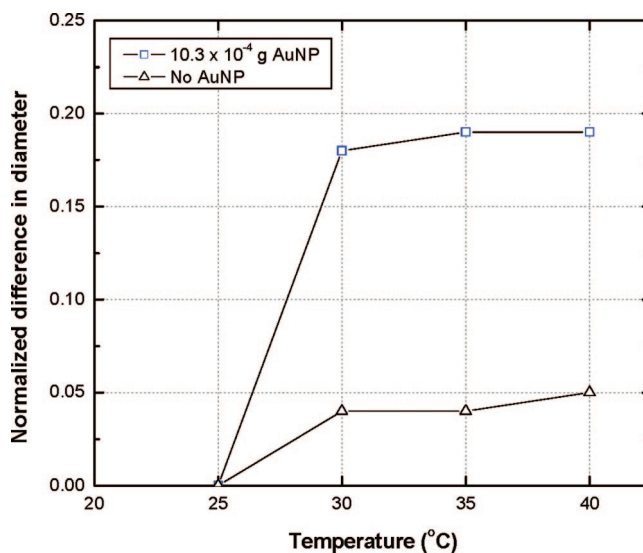


Figure 2. Variation in *normalized difference in diameter* as a function of temperature for PNIPAm-*co*-Am microgels loaded with 10.3×10^{-4} g AuNPs (□) and no AuNPs (Δ). The continuous phase was water.

(28) Budhlall, B. M.; Marquez, M.; Velev, O. D. *Langmuir*, in press.

(29) Heskings, H.; Guillet, J. E. *J. Macromol. Sci. Chem. A* **1968**, *2*, 1441–1455.

(30) Iwai, K.; Hanasaki, K.; Yamamoto, M. *J. Lumin.* **2000**, *87–89*, 1289–1291.

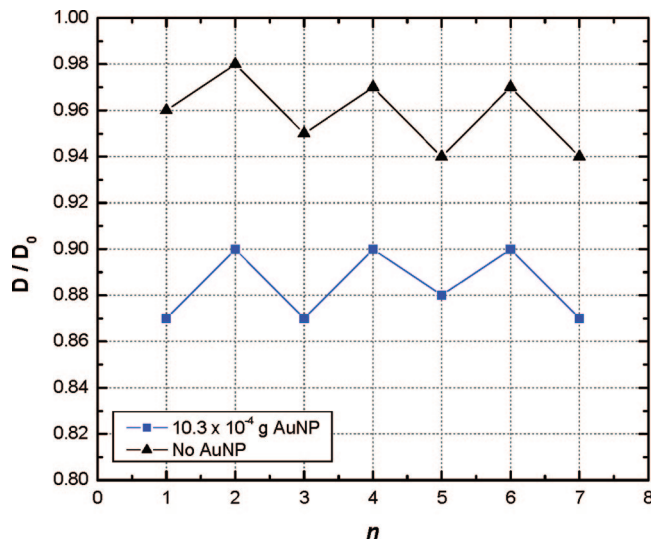


Figure 3. Variation in deswelling ratio, D/D_0 , as a function of the number of heating-cooling cycles, n , between 40 and 30 °C for PNIPAm-co-Am microgel loaded with 10.3×10^{-4} g AuNPs (■) and no AuNPs (▲). D_0 is the average diameter of the microgel at 30 °C (obtained after 5 min equilibrium); D is the average diameter following 5 min equilibrium at 40 °C. The continuous phase was water.

taken after a fixed period of time (15 s after the stop of heating) for the PNIPAm-co-Am microgels with and without AuNPs, a smaller diameter (corresponding to a higher normalized difference in diameter shown in Figure 2) is measured for the microgels with AuNPs. One can hypothesize that localized heating of the AuNPs and dissipation of heat to the polymer by conduction allows the polymer matrix to remain at temperatures, $T > LCST$ for a longer period. This higher temperature may allow the coils to be in the collapsed state longer resulting in a greater extent of shrinkage for the microgels with AuNPs. While this kinetic hypothesis was not tested, a more plausible origin of this surprising effect is that the nanoparticles serve as sites that initiate and nucleate the polymer chain collapse. The phase transition from swollen to collapsed state in PNIPAm is due to changes in the balance of the hydrophobic and hydrophilic bonding states.³¹ Schild reported that this is due to a two-stage process involving an intramolecular coil collapse upon heating to temperatures above LCST, followed by aggregation of the collapsed coils.⁶

Another plausible hypothesis for the greater shrinkage in the presence of AuNPs is that the AuNPs facilitate the cross-linking of polymer chains, which are adsorbed around them, resulting in a larger mechanical stress and stronger collapse of the polymer chains. The two effects are not mutually exclusive, and the results indicate that AuNPs could be used in making more strongly responsive microgels and hydrogels.

The relative degree of shrinkage of the microgels is indicated by the deswelling ratio, D/D_0 , where D_0 is the average diameter of the microgel at 30 °C obtained after 5 min and D is the average diameter following 5 min at 40 °C. Five minutes was chosen as a fixed time-period between cycles to allow the microgels to reach thermal equilibrium. The experimental results of cyclic deswelling-swelling of PNIPAm-co-Am microgels with and without AuNPs are shown in Figure 3, following alternating heating-cooling cycles, (where n represents 1/2 cycle) between 40 and 30 °C. A slightly smaller size of hybrid AuNP/PNIPAm-

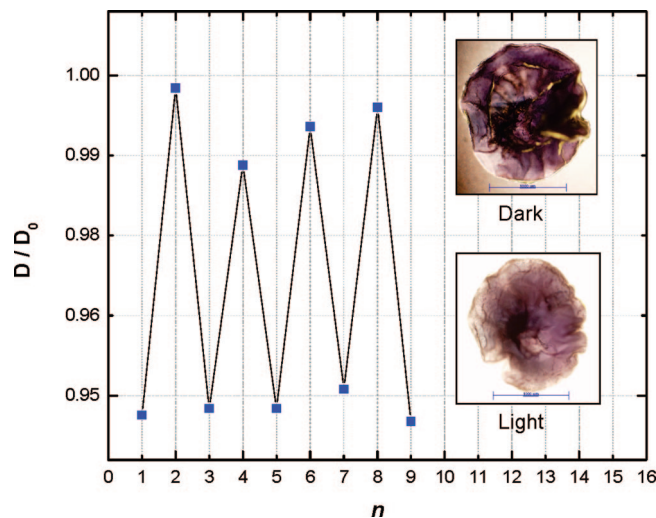


Figure 4. Variation in deswelling ratio, D/D_0 , as a function of the number of light exposure cycles, n , via alternating between a phase-contrast filter and a bright-field filter under an optical microscope for PNIPAm-co-Am microgels loaded with 10.3×10^{-4} g AuNPs. D_0 is the average diameter of the microgel under the phase-contrast filter (obtained after 5 min equilibrium); D is the average diameter following 5 min exposure to the bright-field filter. Insert: optical images of microgel exposed under a phase-contrast filter (dark) and a bright-field filter (light) for 5 min respectively. The continuous phase was mineral oil.

co-Am microgel and a similar deswelling behavior of the PNIPAm-co-Am with and without AuNPs were observed. However, the extent of shrinkage of the AuNP/PNIPAm-co-Am microgels was significantly greater than that of the PNIPAm-co-Am without AuNPs. The water recovery of each microgel is almost 100%, facilitating a somewhat reversible and repeatable temperature response regardless of whether or not AuNP is present. The reason for this recovery of the size of the microgels after each heating-cooling cycle is that the polymer chains undergo intra- and intermolecular H-bonding with water rapidly facilitating a coil-to-globule transition when the microgels are exposed to heating-cooling cycles between 40 and 30 °C.

Effect of Light Irradiation. The effect of light irradiation on PNIPAm-co-Am microgels without AuNPs and with AuNPs at the same loading of 10.3×10^{-4} g AuNPs as in the temperature variation experiment was studied. The gels were dispersed in a continuous phase of mineral oil. We irradiated the microgels with visible light in order to investigate the influence of visible light actuation on the response of the PNIPAm-co-Am microgel. In the first series of experiments with light actuation, the microgels were placed into the concave wells of the microslides. These microslides were then placed on the sample stage of an optical microscope for irradiation and observations. They were then subjected to light exposure alternating between a phase-contrast filter and a bright-field filter.

The variation in deswelling ratio, D/D_0 , as a function of the number of light exposure cycles, n , for PNIPAm-co-Am microgels is shown in Figure 4. D_0 is the average diameter of the microgel under the phase-contrast filter obtained after 5 min and D is the average diameter following 5 min exposure to the bright-field filter. The inserts in Figure 4 shows optical micrographs of photothermally triggered volume phase transitions of the AuNP/PNIPAm-co-Am microgel exposed under a phase-contrast filter (dark) and a bright-field filter (light) for 5 min respectively. The light exposure cycles, n are repeated more than 8 times and show that the photothermal response is reversible and reproducible. The reversibility of the response also shows that the microgel

(31) (a) Heskins, M.; Guillet, J. E. *J. Macromol. Sci. Chem. A* **1968**, *2*, 1441–1445. (b) Fudjishige, S.; Kubota, K.; o, I. *J. Phys. Chem.* **1989**, *93*, 3311–3313. (c) Winnik, F. M. *Polymer* **1990**, *31*, 2125–2134. (d) Wang, X.; Qiu, X.; Wu, C. *Macromolecules* **1998**, *31*, 2972–2976.

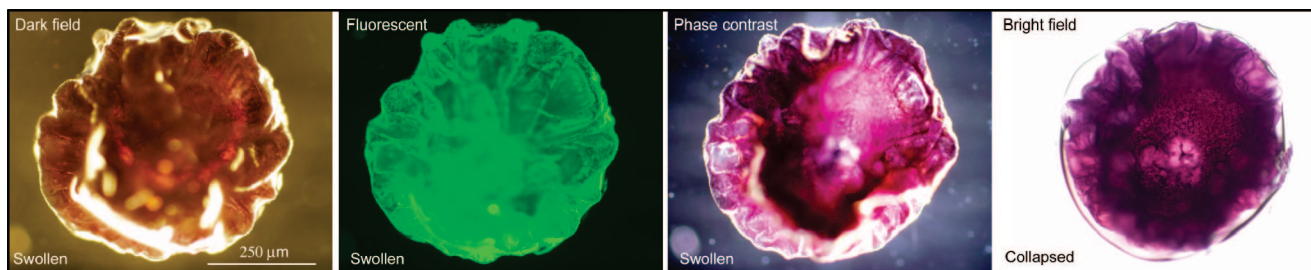


Figure 5. Optical micrographs for PNIPAm-*co*-Am microcapsules loaded with 10.3×10^{-4} g AuNPs. The images were taken after 5 min equilibrium under each filter. Under the dark field, fluorescent and phase contrast filters (*dark*) the microgel appear as a “swollen” polymer shell containing colloidal AuNPs homogeneously dispersed within the microgel, whereas under the bright field filter (*light*) the microgel collapsed, shrank in size, and excluded water from the core and interstitial spaces from the within the polymer matrix.

shrinkage does not lead to irreversible phase separation of the AuNPs inside the polymer.

The shrinkage is due to visible light exciting the AuNPs at its resonance frequency, and the resulting conversion of this light energy to heat locally within the polymer microgel shell; when the temperature increases to or above LCST, the microgel will collapse or shrink as shown. A movie illustrating the dynamics of photothermally triggered deswelling–swelling volume phase transition is available in the Supporting Information. In the control experiment, with no AuNPs present in the PNIPAm-*co*-Am microgel, no visible shrinkage occurs.

The next series of experiments involved exposing the microgels to light beams of varying wavelengths and intensities. Optical micrographs for PNIPAm-*co*-Am microgels loaded with 10.3×10^{-4} g AuNPs are shown in Figure 5. A fluorescent dye, FITC, was incorporated with the monomer in the aqueous phase prior to photopolymerization of the microgel. Microgels without light-absorbing AuNPs were similarly irradiated as a control experiment with no shrinkage observed. Under the dark field, fluorescent and phase contrast filters (*dark*) the microgels appear as a “swollen” polymer shell containing colloidal AuNPs homogeneously dispersed within the microgel. However, under the bright field filter (*light*) the microgel collapsed, shrank in size and excluded water from the core and interstitial spaces from within the polymer matrix. Since the microgels without light-absorbing AuNP showed no shrinkage, this confirmed that the visible light exposure had no apparent effect on the morphology of the microgels without the light-absorbing AuNPs in their polymer matrix. The absorption of light by the AuNPs appears to be key in increasing the temperature of the polymer matrix to $T > \text{LCST}$ resulting in shrinkage in size as the polymer chains become more hydrophobic.

These light experiments demonstrate that the hybrid AuNP/PNIPAm-*co*-Am microgels can be actuated by visible light at exposure intensities well below those used in current medical techniques.³² It has been reported that in laser skin treatment and tattoo removal, exposures of up to 650 mJ/cm^2 are applied.³³ It is envisioned that this microgel system can have potential applications to microfluidic switches or microactuators, photosensors, and various nanomedicine applications in controlled delivery and release.

Effect of Microwave Irradiation. The effect of microwave irradiation on PNIPAm-*co*-Am microgels was studied in the next series of experiments. The microgels without and with AuNPs loaded were dispersed in a continuous phase of *mineral oil*. The effect of AuNPs concentration on the volume phase transition of the PNIPAm-*co*-Am microgel on exposure to microwave

irradiation was also studied. A corresponding study in *water* as the continuous phase was also conducted. Low applied microwave power should result in localized heating below the pain threshold^{22a} and water evaporation temperatures.²³ The effects of microwave power on the microgels were evaluated at different exposure times of 15, 30, 45, 60, 120 and 180 s, which corresponded to maximum microwave energy of 0.21, 0.42, 0.64, 0.85, 1.69 and 2.54 kJ/m^3 respectively. The volume of water and oil exposed was $\sim 1 \text{ cm}^3$. The behavior of these microgels suspended in mineral oil is illustrated in Figure 6. In general the microgels decreased in size as the microwave irradiation increased, indicating an increased power dissipated to the AuNP/PNIPAm-*co*-Am particles. There is a threshold microwave exposure for which the microgels shrank in size and excluded water from the core and interstitial spaces from within the polymer matrix. For the AuNPs loaded PNIPAm-*co*-Am it is after 45 s of microwave heating corresponding to 0.64 kJ/m^3 compared to the control PNIPAm-*co*-Am microgel without AuNPs where it is after 180 s at 2.54 kJ/m^3 .

This rapid reduction in size is quantitatively presented in Figure 7 where the *normalized difference in diameter* is plotted as a function of microwave time. The AuNPs influence the ability and extent to which the microgels collapse and swell as seen from 33% shrinkage for the microgel with 10.3×10^{-4} g AuNPs compared to 7% shrinkage for the control experiment without AuNPs for the same exposure of 45 s. In addition, the concentration of AuNPs loading within the microgel increases the extent of collapse from 16% for the microgel with 2.8×10^{-4} g AuNPs compared to 33% for the microgel at a higher AuNPs loading of 10.3×10^{-4} g.

Having established the threshold exposure of 0.64 kJ/m^3 (microwave time of 45 s) for shrinkage and collapse for the microwave induced volume phase transitions of the AuNP/PNIPAm-*co*-Am microgels, we proceeded to determine the repeatability of the deswelling and swelling processes in mineral oil. The variation in deswelling ratio, D/D_0 , as a function of the number of microwave irradiation events n , cycled on and off every 60 s for PNIPAm-*co*-Am microgels loaded with and without AuNPs is shown in Figure 8. As can be expected from the previous results, the control experiment with no AuNPs showed very little shrinkage after cycling on and off every 60 s of microwave irradiation for seven cycles ($n = 7$). In contrast, the deswelling–swelling cycle induced by the on–off switching of the microwave irradiation could be repeated more than 6 times for the AuNP/PNIPAm-*co*-Am microgels. Of significant interest is the dampening of the magnitude of the deswelling–swelling ratio as the number of cycles increased. It is postulated that this dampening effect is due to phase separation and evaporation of water from the microgels, making less water available for

(32) Jacques, S. L. *Surg. Clin. North. Am.* **1992**, 72, 531–558.

(33) Radt, B.; Smith, T. A.; Caruso, F. *Adv. Mater.* **2004**, 16, 2184–2189.

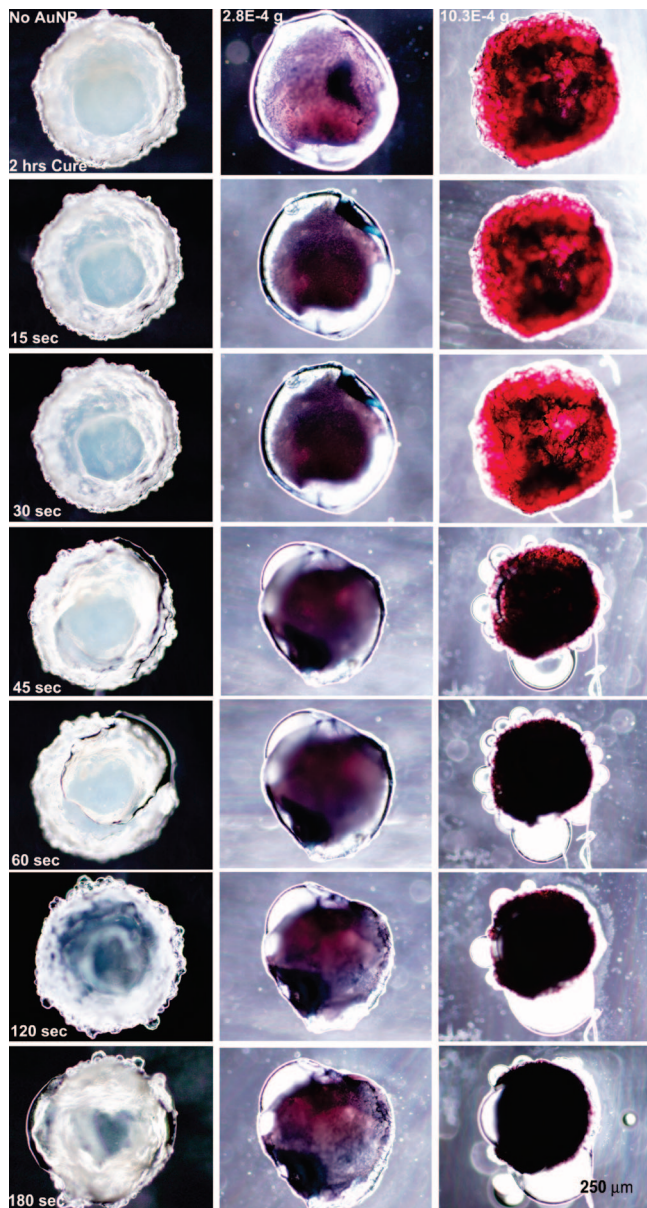


Figure 6. Optical micrographs of PNIPAm-co-Am core-shell microgels after photopolymerization via 2 h of UV exposure and increasing microwave irradiation times. PNIPAm-co-Am microcapsule loaded with 2.8×10^{-4} AuNPs shows a red core comprised of AuNPs with a clear shell of polymer. 10.3×10^{-4} g AuNPs loaded microgel shows a homogeneous distribution of AuNPs throughout the polymer microgel. The subsequent rows show the optical micrographs of PNIPAm-co-Am core-shell microgels without AuNPs and with varying concentration of AuNPs (horizontal directions) and varying microwave irradiation times (vertical direction). The continuous phase was *mineral oil*.

hydrophilic interactions of the polymer chains as the number of microwave events increased.

The corresponding microwave irradiation experiments in *water* (compared with the *mineral oil* experiments) resulted in similar differences between the low concentration (2.8×10^{-4} g AuNPs) AuNP/PNIPAm-co-Am microgels and the control experiment without AuNPs and are shown in Figures 9 for *water* and in Figure 7 for *mineral oil*. However, in *water*, there is a larger difference in the shrinkage and collapse when higher AuNPs concentration (10.3×10^{-4} g AuNPs) is loaded in the PNIPAm-co-Am as observed by a ~ 2 -fold reduction in size of the microgels compared to the PNIPAm-co-Am loaded with 2.8×10^{-4} g AuNPs.

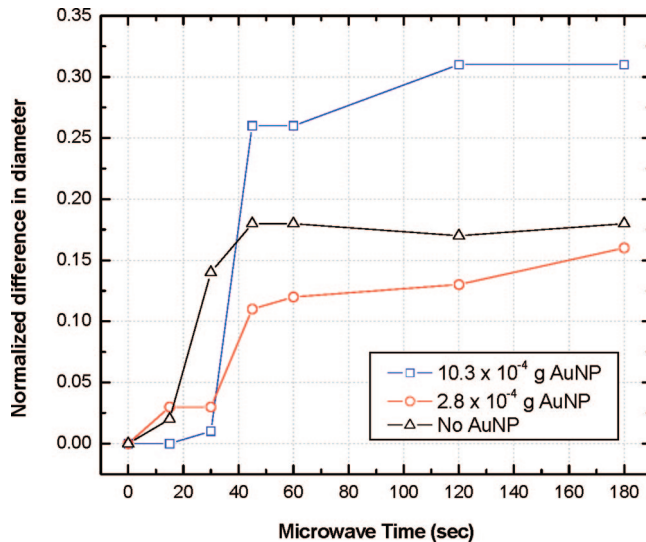


Figure 7. Variation in normalized difference in diameter as a function of microwave irradiation time for PNIPAm-co-Am microgels loaded with 2.8×10^{-4} g AuNPs (○) 10.3×10^{-4} g AuNPs (□) and no AuNPs (Δ). The continuous phase was *mineral oil*.

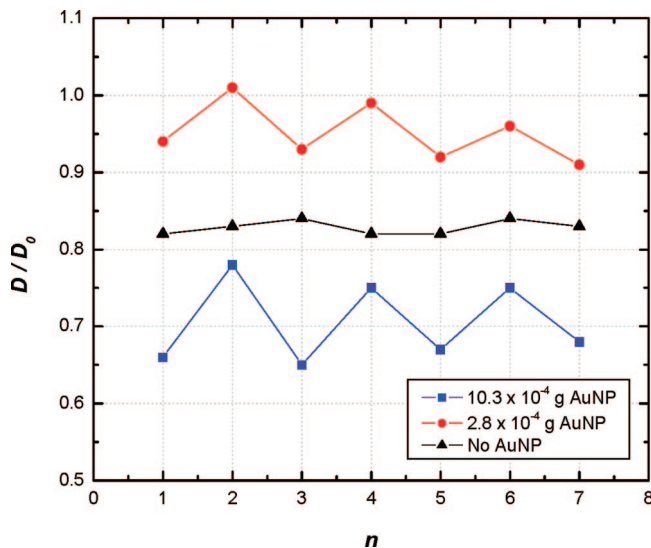


Figure 8. Variation in deswelling ratio, D/D_0 , as a function of the number of microwave events for 60 s, n for PNIPAm-co-Am microgels loaded with 2.8×10^{-4} g AuNPs (●) 10.3×10^{-4} g AuNPs (■) and no AuNPs (▲). D_0 is the average diameter of the microcapsule under ambient laboratory conditions at 22 °C (obtained after 5 min equilibrium); D is the average diameter following microwave irradiation. The continuous phase was *mineral oil*.

A plausible explanation for these results is that the microwave absorption of the continuous phase plays a significant role in the heating of the microgels. The relatively high microwave absorption of water and mineral oil allows the control microgel without AuNPs to heat to a similar extent as the low concentration of AuNP/PNIPAm-co-Am microgel. It is only when a significantly higher concentration of AuNPs is loaded in the microgel that there is a significant reduction in the size of the particle.

The role of the continuous phase is further illustrated when the deswelling-swelling experiments are conducted in *water* (Figure 10) compared to *mineral oil* (Figure 8). The variation in deswelling ratio, D/D_0 , as a function of the number n corresponded to microwave switching on and off every 60 s. The microwave induced deswelling-swelling transitions in AuNP/PNIPAm-co-Am microgels in *water* were reversible with no

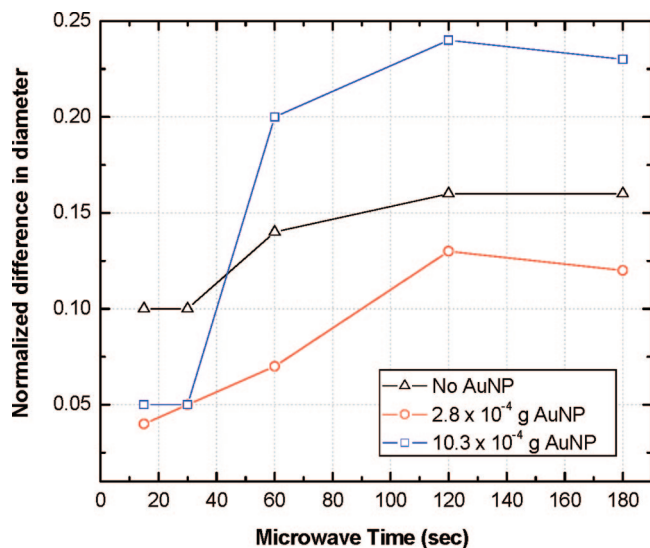


Figure 9. Variation in normalized difference in diameter as a function of microwave time for PNIPAm-co-Am microgels loaded with 2.8×10^{-4} g AuNPs (○) 10.3×10^{-4} g AuNPs (□) and no AuNPs (Δ). The continuous phase was water.

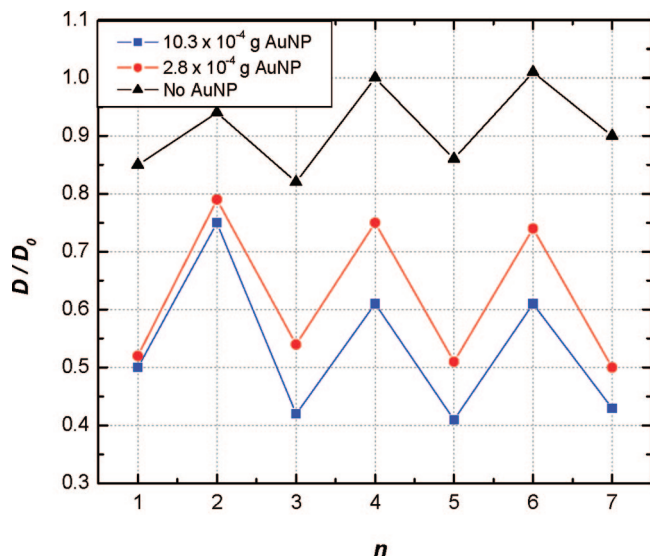


Figure 10. Variation in deswelling ratio, D/D_0 , as a function of the number of microwave events for 60 s, n for PNIPAm-co-Am microgels loaded with 2.8×10^{-4} g AuNPs (●) 10.3×10^{-4} g AuNPs (■) and no AuNPs (▲). D_0 is the average diameter of the microgel under ambient laboratory conditions at 22 °C (obtained after 5 min equilibrium); D is the average diameter following microwave irradiation. The continuous phase was water.

dampening in the cycle as the number of on and off events increased, in contrast to when *mineral oil* is used as the continuous phase (Figure 8). These results were expected as in *water*, all the polymer microgels are able to recover $\sim 100\%$ from the replenishment of water in the continuous surrounding phase which acts as a reservoir. The presence of AuNPs in the microgels increases the degree of deswelling-swelling because of localized heating of the polymer matrix by the AuNPs, however, there were marginal differences between AuNP/PNIPAm-co-Am microgels at the concentrations, 2.8×10^{-4} and 10.3×10^{-4} g AuNPs studied.

A direct comparison of the effect of microwave irradiation and the effect of temperature, both conducted in water, on the

AuNP/PNIPAm-co-Am microgels cannot be made, as the microgels may not have been in thermodynamic equilibrium when the respective measurements were taken. In principle, comparisons can be made only if the temperature profiles of the microgels were measured immediately after microwave irradiation; however, because of the rapid collapse (within 45 s) and reswelling of the particles, micrographs and temperature measurements could not be taken simultaneously. To the best of the authors' knowledge, this is the first report of microwave-driven actuation of AuNP loaded PNIPAm-co-Am microgels.

Conclusions

We successfully demonstrated use of our combined synthesis strategy of liquid-liquid phase separation and a double emulsion microarray technique to prepare *stimuli*-responsive hybrid AuNP/PNIPAm-co-Am microgels. The evidence for this is shown in Figure 5. There is a striking contrast of the fluorescently (FITC dye) labeled polymer-shell in green with the dark red core of the encapsulated colloidal AuNPs with the completely black (no fluorescent label) continuous phase of mineral oil. Additional evidence for a high *efficiency* encapsulation of mineral oil in the core is the fact that there is such a striking contrast in the fluorescent image; this indicates that there is no leak of fluorescence into the continuous phase. The microarray technique used to perform the experiments is rapid and robust and the process can be scaled up relatively easily for fabricating large quantities of AuNP/PNIPAm-co-Am microgels.

AuNP/PNIPAm-co-Am microgels showed a dramatic decrease in volume in *mineral oil* and *water* compared to PNIPAm-co-Am microgels without AuNPs when actuated by visible light, microwave radiation and temperature. The photoresponsive behavior of the AuNP/PNIPAm-co-Am microgels is dependent on the intensity and wavelength of the irradiated light. The microwave deswelling-swelling behavior is dependent on the microwave absorption of the continuous phase and the concentration of AuNPs in the thermoresponsive PNIPAm-co-Am microgel. This study demonstrated that AuNP/PNIPAm hybrid core-shell microgels can be actuated by visible light and microwave radiation (< 1250 nm) and temperature. In addition, this is the first study to demonstrate that incorporating AuNPs speeds up the response kinetics of PNIPAm, and hence enhances the sensitivity to external stimuli of PNIPAm. The liquid core of the polymer microcapsule can be released by activation of a range of electromagnetic radiation (visible light and microwave) and temperature, suggesting this novel microgel may have potential applications in microfluidic switches or microactuators, photosensors, and in controlled delivery and release.

Acknowledgment. B.M.B. acknowledges the University of Massachusetts, Lowell, for granting time to work with Prof. Velev, International Network of Emerging Science and Technology Group, Phillip Morris USA for funding, Emily Hon (undergraduate student), Suk-Tai Chang and Ketan Bhatt (graduate students) for performing some of the experiments and providing training on the confocal microscope, respectively.

Supporting Information Available: Synthesis and characterization of AuNPs showing TEM images and UV-vis spectra. A movie showing the dynamics of photothermally triggered deswelling-swelling volume phase transition of the PNIPAm-co-Am microgel containing AuNPs. This material is available free of charge via the Internet at <http://pubs.acs.org>.